Technical University of Denmark

**DTU**

# Topology optimization of devices for wireless energy transfer

The design parametrization

**Aage, Niels; Mortensen, N. Asger; Sigmund, Ole**

*Published in:*
8th World Congress on Structural and Multidisciplinary Optimization

*Publication date:*
2009

*Document Version*
Early version, also known as pre-print

Link back to DTU Orbit

*Citation (APA):*
Aage, N., Mortensen, A., & Sigmund, O. (2009). Topology optimization of devices for wireless energy transfer: The design parametrization. In 8th World Congress on Structural and Multidisciplinary Optimization

**DTU Library**
Technical Information Center of Denmark

# Topology optimization of devices for wireless energy transfer
# The design parametrization

## N. Aage, N.A. Mortensen, O. Sigmund

Technical University of Denmark, Solid Mechanics, Kgs. Lyngby, Denmark. Email: naa@mek.dtu.dk
Technical University of Denmark, Photonics Engineering, Kgs. Lyngby, Denmark. Email: namo@fotonik.dtu.dk
Technical University of Denmark, Solid Mechanics, Kgs. Lyngby, Denmark. Email: sigmund@mek.dtu.dk

## 1. Abstract

In electromagnetic optimization problems involving metallic microwave devices, such as resonators for wireless energy transfer, the volumetric distribution of good conductors, e.g. copper, have been known to cause numerical bottlenecks. In finite element analysis the limiting factor is the so-called skin depth, which calls for highly refined meshing to capture the physics. This has until now prohibited the application of topology optimization to such problems. In this paper we present a design parametrization that remedies this numerical bottleneck by interpolating between Maxwell's equations and an element impedance condition. The proposed design parametrization is confirmed by numerical examples.

**2. Keywords:** topology optimization, conductor design, finite elements, Maxwell's equations.

## 3. Introduction

The motivation for this work originates from the ever increasing usage of small handheld, or autonomous, electrical devices. Such devices, apart from their distinct functionality, share some general design issues. The devices used for communication relies heavily on an efficient antenna, confined within the geometric specifications of the device. A typical antenna is a metallic device connected to a transmission line [1]. However, common for all small electrical devices is that they consume energy. This ultimately means that the devices are no better than their power supplies allow them to be. The solution to the power problem took a new turn in 2007, where a MIT group lead by Prof. M.Soljacic demonstrated that one could obtain efficient mid-range wireless energy transfer (WiTricity) using magnetically resonant coupled copper coils [2]. The design of antennas and the design of transmitters/receivers for WiTricity, are therefore obvious candidates for the topology optimization method.

Topology optimization has proven to be a very successful design tool for general mechanical problems [3, 4]. Also in electromagnetic (EM) problems involving distribution of dielectric materials, e.g. dielectric antennas [7] and photonic crystals [5], the method has been applied with success. This work contributes with knowledge on how to obtain a numerically efficient topology optimization method for EM problems involving the distribution of a good conductor, such as copper, in the radio frequency (RF) range, i.e. 3 Hz to 300 GHz.

Previous work conducted on the subject is sparse due to the aforementioned numerical bottleneck, and the fact that until very recently, standard antenna designs and power supplies were adequate for almost all applications. However, in [8] the authors demonstrates the possibilities of applying gradient based topology optimization to the design of conformal electrically small antennas [1]. Though successful, the authors addresses the skin depth problem as a limiting factor, which should be remedied. Others, such as [9], have used generic algorithms (GA) for the volumetric distribution of copper in antenna design problems. Also here the authors obtain good designs, but are limited by the combinatoric approach used in GA.

### 3.1. Paper Outline

The remainder of this paper is organized as follows. First the governing equations and conductor modeling relevant for the development of the design parametrization is introduced. Next the finite element equations are discussed. The design parametrization is then introduced based on ideas from EM modeling in relation with the weak form. The proposed design parametrization is then confirmed by numerical examples. Finally the findings are summarized.

## 4. Physical & Numerical Model

In this section the governing equations necessary for the development of the design parametrization will

be introduced. This includes Maxwell's vector wave equation, the associated weak form along with the impedance condition.

### 4.1. Maxwell's Equations

Maxwell's equations for a linear, isotropic medium with no free charges, can be cast in the frequency domain assuming time-harmonic waves using the time convention $\boldsymbol{u}(\boldsymbol{x}, t) = \mathbb{R}\left[\boldsymbol{u}(\boldsymbol{x})e^{j\omega t}\right]$, where $\omega$ is the frequency, $j$ represents the imaginary unit and $\mathbb{R}(\cdot)$ is the real part [10]. By trivial manipulations, the set of first order partial differential equations (PDEs), can be recast as a single second order PDE in either the electric field, $\boldsymbol{E}$, or the magnetic field, $\boldsymbol{H}$. For the electric field it can be stated as

$$\nabla \times \left[\mu_r(\boldsymbol{r})^{-1}\nabla \times \boldsymbol{E}\right] - k_0^2 \epsilon_c(\boldsymbol{r})\boldsymbol{E} = \boldsymbol{0} \tag{1}$$

where $\boldsymbol{r}$ is the position, $k_0 = \omega\sqrt{\epsilon_0\mu_0}$ is the free space wave number, $\epsilon_0$ is the free space permittivity and $\mu_0$ the free space permeability. The material specific parameters $\mu_r(\boldsymbol{r})$ and $\epsilon_c(\boldsymbol{r})$ are the relative permeability and relative complex permittivity respectively. The complex permittivity is given by

$$\epsilon_c(\boldsymbol{r}) = \epsilon_r(\boldsymbol{r}) - j\frac{\sigma(\boldsymbol{r})}{\omega\epsilon_0} \tag{2}$$

where $\epsilon_r(\boldsymbol{r})$ is the dielectric function and $\sigma(\boldsymbol{r})$ is the electric conductivity. With respect to the topology optimization problem, the position dependent material parameters, $\mu_r(\boldsymbol{r})$, $\epsilon_r(\boldsymbol{r})$ and $\sigma(\boldsymbol{r})$ are the unknown functions to be determined.

### 4.2. Impedance Condition

Before presenting the weak form, or finite element form, of the vector wave equation the notion of skin depth is introduced. In EM wave propagation the skin depth, $\delta$, is a measure for the distance through which the amplitude of a traveling plane wave decreases by a factor $e^{-1}$ in a conductor [1]. An approximation can be obtained through the following formula

$$\delta = \frac{1}{\sqrt{\pi\sigma\mu\omega}} \tag{3}$$

The skin depth is important since most microwave devices have sizes in the order of $mm$, while the skin depth typically is in the $\mu m$ range, i.e. three orders of magnitude smaller. To put skin depth into the context of finite elements and topology optimization, let us consider an example in which we wish to use a small cube of $2 \times 2 \times 2$cm for design domain. The target frequency is set to 300 MHz and the conductor is chosen to be copper with $\sigma = 5.998 \cdot 10^7$S/m. In that case the skin depth becomes $\delta = 3.8 \cdot 10^{-6}$m. For topology optimization each element in the mesh is possibly metallic, and thus the whole domain must be meshed such that the skin depth can be resolved. Using simple first order finite elements one should have at least two elements per skin depth to capture the rapid decay. This leads to approximately 10.000 elements in each spatial direction, i.e. a total of $10^{12}$ elements in 3D. Such numbers of elements implies that direct interpolation, as done in most other topology optimization problems [4], is insufficient for the microwave problem.

Due to the skin depth issue most numerical modeling of metallic devices utilizes boundary conditions to represent the conducting regions. For perfect electric conductors (PEC), i.e. $\sigma = \infty$, the skin depth is zero, and the metal can be modeled by a homogenous Dirichlet condition for the electric field and a homogenous Neumann condition for the magnetic field. For finite conductivity an approximate relation between the electric and magnetic fields can be used, which can be stated as a mixed boundary condition on the same form for both fields [11]. Below the approximate condition is stated for the electric field

$$\boldsymbol{n} \times \left([\mu_r^d]^{-1}\nabla \times \boldsymbol{E}\right) + jk_0\sqrt{\frac{\epsilon_c^m}{\mu_r^m}}\boldsymbol{n} \times (\boldsymbol{n} \times \boldsymbol{E}) = \boldsymbol{0} \tag{4}$$

where $\boldsymbol{n}$ is normal vector pointing into the conductive region, $(\cdot)^d$ and $(\cdot)^m$ refer to the dielectric and the metal respectively. Note that an equivalent formulation can be derived for the magnetic field form of Maxwell's equations. The condition in Eq.(4) is called an impedance conditions, and it forms the backbone for the material interpolation scheme to be presented in the upcoming chapter.
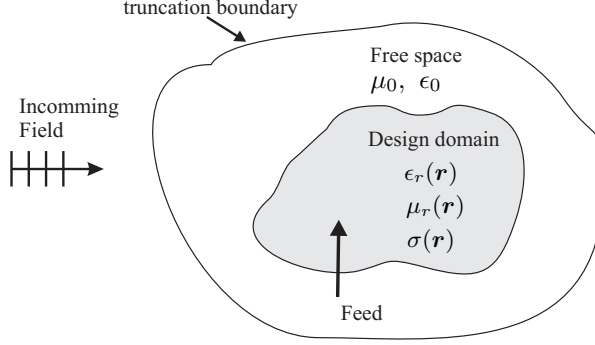
### 4.3. Weak Formulation

Figure 1: Illustration of a general EM topology optimization problem which can be used for the design of microwave antennas, magnetic resonators, etc.

In this section the numerical solution to Maxwell's vector wave equation is addressed. Numerical methods, such as integral methods, finite elements and finite differences, could all be used for the Maxwell problem, but due to geometric freedom and sparsity of system matrices the finite element method is preferred and used in the work presented here.

The finite element formulation, or weak form, can for obvious reasons not determine the solution to Maxwell's equations in infinite space. Therefore the domain of interest is truncated and some approximation to the Sommerfeld radiation condition [10] is applied at this boundary. The most frequently used numerical techniques for truncation includes absorbing boundary conditions (ABC), perfectly matched layers (PML) and finite element boundary integral (FE-BI) methods [11]. A general sketch of an analysis problem including optimization can be seen in figure 1. Let $\Omega$ be the total computational domain, and $\Gamma$ the truncation boundary. For e.g. the electric field the problem becomes to find $\boldsymbol{W} \in H_0(\text{curl}, \Omega)$

$$\int_\Omega \left[ (\nabla \times \boldsymbol{W}) \cdot \mu_r^{-1} \cdot (\nabla \times \boldsymbol{E}) - k_0^2 \boldsymbol{W} \cdot \epsilon_c \cdot \boldsymbol{E} \right] \mathrm{d}\Omega$$

$$- \int_\Gamma \boldsymbol{W} \cdot \left[ \boldsymbol{n} \times \left( \mu_r^{-1} \cdot \nabla \times \boldsymbol{E} \right) \right] \mathrm{d}\Gamma = 0 \qquad (5)$$

$$\forall \boldsymbol{E} \in H(\text{curl}, \Omega)$$

where $\boldsymbol{W}$ is a vector test function. For more details on the vector, or edge, based finite elements associated with the function space $H(\text{curl}, \Omega)$ the reader is referred to e.g. [11, 12]. The surface integral in Eq. (5) means that the discrete form, or FE equations, depends on the specific boundary condition applied on $\Gamma$. Therefore, and not to loose generality, the discrete form will not be specified until the presentation of a numerical example.

**5. Design Parametrization**

The design parametrization presented next follows the standard topology optimization approach in which each element in the finite element mesh is associated with a continuous design variable, or density, $0 \le \rho^e \le 1$. The design variable is used to interpolate between candidate materials which in this setting is a conductor, $(\cdot)^m$, and a dielectric $(\cdot)^d$. Intermediate values of the design variables are unwanted since these are difficult to interpret physically and thus makes the optimized designs hard to fabricate. Therefore the interpolation functions must be chosen such that regions of intermediate densities are minimized.

5.1. Design Dependence in Maxwell's Equations

In order to circumvent the limitations induced by the skin depth problem, the design parametrization is based on a mixture of Maxwell's equations and an element impedance condition. This is to be understood as if each element of conducting material is replaced by an impedance condition. For a single design element this can be stated generally without specifying the interpolation functions as

$$\begin{aligned} \nabla \times (\tilde{A}\nabla \times \boldsymbol{u}) - k_0^2 \tilde{B}\boldsymbol{u} &= 0, & \text{in } \Omega^e \\ \boldsymbol{n} \times (A\nabla \times \boldsymbol{u}) - f(\rho^e) jk_0\sqrt{AB}\boldsymbol{n} \times (\boldsymbol{n} \times \boldsymbol{u}) &= 0, & \text{on } \Gamma^e \end{aligned} \qquad (6)$$

3

Table 1: Field dependent parameters for the design parametrization used for conductor/dielectric based topology optimization, Eqs.(6). The superscripts $(\cdot)^d$ refer to the dielectric and $(\cdot)^m$ to the metal. The functions $\mu_r(\rho^e)$, $\epsilon_r(\rho^e)$ and $\sigma(\rho^e)$ is given in Eq. (7).

| $\boldsymbol{u}$ | $A$ | $B$ | $\tilde{A}$ | $\tilde{B}$ |
|---|---|---|---|---|
| $\boldsymbol{E}$ | $(\mu_r^m)^{-1}$ | $\epsilon_r^m - j\frac{\sigma^m}{\omega\epsilon_0}$ | $\mu_r(\rho^e)^{-1}$ | $\epsilon_r(\rho^e) - j\frac{\sigma(\rho^e)}{\omega\epsilon_0}$ |
| $\boldsymbol{H}$ | $\left(\epsilon_r^m - j\frac{\sigma^m}{\omega\epsilon_0}\right)^{-1}$ | $\mu_r^m$ | $\left(\epsilon_r(\rho^e) - j\frac{\sigma(\rho^e)}{\omega\epsilon_0}\right)^{-1}$ | $\mu_r(\rho^e)$ |

where $\Omega^e$ and $\Gamma^e$ refer to the element volume and boundary respectively, and $\boldsymbol{n}$ is an outward normal for element $e$. The dependent field $\boldsymbol{u}$ and its associated parameters $A$, $B$, $\tilde{A}$, $\tilde{B}$ are given in table 1. Note that the sign in the impedance condition has changed, since the normal now points into the element. The function $f(\rho^e)$ is included to control the presence of the element impedance condition. When $f(\rho^e) = 0$ only the first term of the element boundary condition in Eq. (6) remains and is equated to zero. With respect to the weak form this means that the boundary integral in Eq. (5) disappears and therefore that the standard wave equation is obtained. For $f(\rho^e) = 1$ the impedance condition is present and the wave equation is suppressed, hence the skin depth is resolved.

Note that this approach does not allow for direct interpolation of the conductivity in the element impedance condition, since for $\sigma = 0$ we have that $\epsilon_c = \epsilon_r$ which means that the element boundary condition does not vanish for $\rho^e = 0$. Also the physical interpretation of intermediate densities is uncertain, though one might be able to link them to materials with varying conductivities. However, if the final design has $\rho = 0$ or $\rho = 1$ in all design elements, the physical performance of the optimized design has been analyzed with a correct physical model. Thus, if the design parametrization is devised such that the final design is black and white, there is no problem in allowing the optimizer to pass through intermediate densities during the iterative optimization process. This is a commonly used trick in topology optimization [4] and will also be used in the work presented here.

5.1. Interpolation Functions

The last step is to determine the interpolation functions identified in Eq.(6) and Table 1. The functions should be chosen such that the following requirements are met best possibly. The interpolation functions must be valid for both the electric and magnetic field formulation of Maxwell's equations. Furthermore, the functions have to be monotonically varying and have the property that a small change in $\rho^e$ should lead to a small change in system response. Finally the interpolation functions should, if possible, result in designs free from intermediate values of $\rho^e$. In some topology optimization problems a penalization parameter is required to obtain black and white designs, as done in e.g. in the Solid Isotropic Material with Penalization (SIMP) scheme, where the stiffness is penalized to make intermediate densities uneconomical [13, 4] for the optimizer. However, as will be explained in the following section the EM optimization problem does not require any type of penalization to ensure black and white designs.

The functions presented below are determined based on numerical studies.

$$
\begin{aligned}
&\mu_r(\rho^e) = \mu_r^d + \rho^e(\mu_r^m - \mu_r^d) \quad &\sigma(\rho) = 10^{\left(\log_{10}(\sigma^d) + \rho^e[\log_{10}(\sigma^m) - \log_{10}(\sigma^d)]\right)} \\
&\epsilon_r(\rho^e) = \epsilon_r^d + \rho^e(\epsilon_r^m - \epsilon_r^d) \quad &f(\rho^e) = \rho_e^{p_{BC}} \\
&p_{BC} \approx 13 \text{ for } \boldsymbol{E} \quad &p_{BC} \approx 1 \text{ for } \boldsymbol{H}
\end{aligned}
\tag{7}
$$

The linear interpolation of the permittivity and permeability is successfully adopted from e.g. [5], while the interpolation function $f(\rho^e)$ and $\sigma(\rho^e)$ needs special attention. Interpolation of the conductivity is made difficult due to the following two reasons. Firstly, the numerical range is huge, i.e. $\sigma = 0$ for free space and $\sigma = 10^7 S/m$ for a typical good conductor [10]. Secondly, the conductivity is a damping parameter for the EM fields. This means that even numerically small conductivities can lead to large changes in field response, and furthermore that conductivities above a certain threshold limit will only have a small influence on the response. Due to these issues it was found that the interpolation of $\sigma$ was best performed in the logarithmic scale, and then converted back to the physical scale using a power function [14]. Finally note that $\sigma^d$ must always be larger than zero, even for lossless dielectrics due to the logarithmic interpolation. For lossless dielectrics we suggest to use $\sigma^d = 10^{-4}$ based on the numerical experiments.
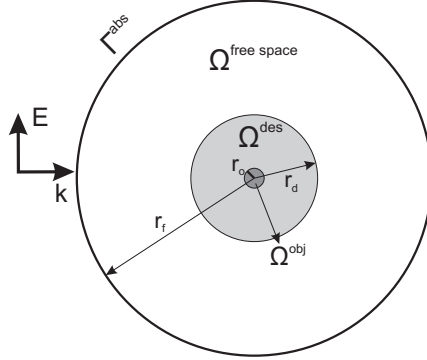
Figure 2: Sketch of the design problem for TE polarized waves. The measures are $r_d = 1.0m$, $r_o = 0.15m$ and $r_f = 2.5m$. The target frequency is 300MHz and the materials are a good conductor e.g. copper and air.

The interpolation function $f(\rho)$ for the element impedance condition must take the difference in field formulation into account. For the electric field the impedance condition is proportional to $\epsilon_c$, while it is proportional to the inverse, i.e. $\epsilon_c^{-1}$, for the magnetic field. From numerical experiments it was found that $f(\rho)$ for the electric field should be similar to a logarithmic function, while $f(\rho)$ should be close to linear for the magnetic field. Since we wish to use the same function for both field formulations, a polynomial with varying exponent is a simple choice, i.e. $f(\rho) = \rho^{p_{BC}}$. The exponent $p_{BC}$, which should not be seen as a penalization parameter c.f. the SIMP scheme [13], yields good results when using $p_{BC} \approx 1$ for the magnetic field and $p_{BC} \approx 13$ for the electric field. The reason why a penalization parameter is not needed for the EM problem is due to damping nature of the conducting material. By this is meant that regions of intermediate conductivities slowly damps, or absorbs, the energy from the EM fields, while a high conductivity means fast damping and thus that less energy is dissipated.

As already stated one can think of the design of electrically conducting devices as the distribution of highly damping material. Due to numerical precision this means that $\sigma^m$ larger than some value, $\sigma^m_{cutoff}$, does not change the system response much. With respect to the optimization a numerically large $\sigma^m$ will then lead to designs with intermediate design variables, since the optimizer won't benefit from letting $\sigma(\rho) \to \sigma^m$. Therefore a study to determine the threshold values of $\sigma^m$ has been conducted. For the electric field the limit was found to coincide with the conductivity of copper, i.e. $\sigma^m_{E_{cutoff}} \approx 10^7 S/m$, while for the magnetic field it was lower, i.e. $\sigma^m_{H_{cutoff}} \approx 10^6 S/m$. Hence, the design parametrization should not be used to distinguish between good conductors such as copper and silver, but should merely be used to model a good conductor.

### 6. Optimization Problem

In this chapter the optimization problem is to be introduced along with its numerical solution. The problem to be considered is the design of a 2D magnetic resonator. This can be seen as a highly simplified model for designing a device for energy harvesting from an incoming EM field. The objective is to maximize the magnetic energy, $\Phi(\rho, \boldsymbol{H}) = \int_{\Omega^{obj}} \mu |\boldsymbol{H}|^2 d\Omega$, in an a priori specified part of the modeling domain, $\Omega^{obj}$, for a target frequency of 300MHz. The design problem is illustrated in figure 2. The model problem assumes transverse electric (TE) polarization, that is

$$
\begin{aligned}
\boldsymbol{H} &= H_z(x,y)\boldsymbol{e}_z \\
\boldsymbol{E} &= E_x(x,y)\boldsymbol{e}_x + E_y(x,y)\boldsymbol{e}_y
\end{aligned}
\tag{8}
$$

which leads to either the scalar Helmholtz equation for the $H_z$ field, or a vector curl-curl equation for the electric field in the plane. To demonstrate that the design parametrization works equally well for both the electric and magnetic formulation, the design problem is solved using both formulations, i.e. nodal elements for $H_z$ and edge elements for $E_x$ and $E_y$ [11]. The modeling domain is truncated with a first order absorbing boundary condition (ABC) located $1.5\lambda$ from the design domain. The complete discrete formulation can now be stated as

$$
(\boldsymbol{S}(\rho) + \boldsymbol{A})\,\boldsymbol{u} = \boldsymbol{f}
\tag{9}
$$

5

(a) $\Phi = 0.41$    (b) $\Phi = 0.37$
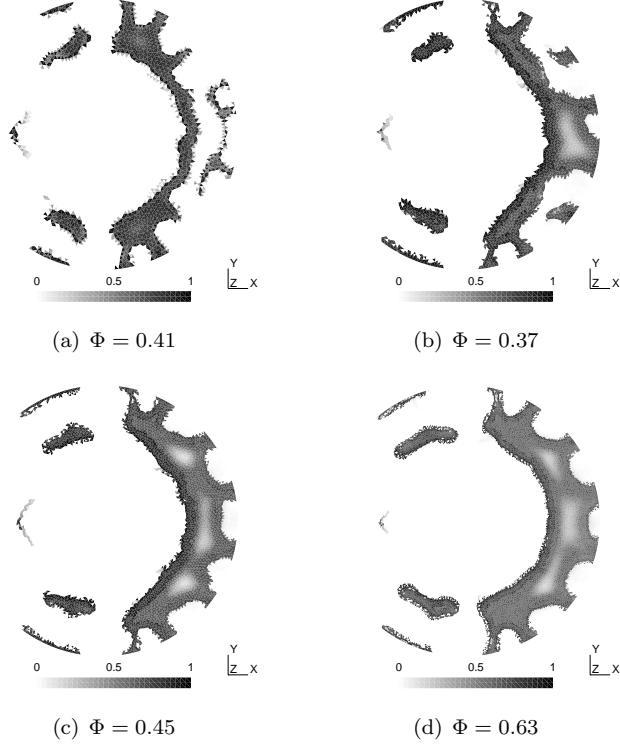
(c) $\Phi = 0.45$    (d) $\Phi = 0.63$

Figure 3: Optimized designs for the problem in figure 2 for three different mesh resolutions with fixed density filter. The number of design elements are (a) 15950 edge elements, (b) 15950 nodal elements, (c) 25292 nodal elements and (d) 41560 nodal elements. Convergence was reached in 120 to 350 iterations.

where $\boldsymbol{S}(\rho)$ refers to the design element contributions, $\boldsymbol{A}$ contains free space, fixed domains and domain truncation contributions and $\boldsymbol{f}$ contains the system load. The system matrix for the design elements can be computed for the electric field formulation as

$$
\begin{aligned}
\boldsymbol{S}(\rho) &= \sum_{e=1}^{N} \left( \boldsymbol{K}^e(\tilde{A}) - \boldsymbol{M}^e(\tilde{B}) - \boldsymbol{B}^e(f(\rho), A, B) \right) \\
\boldsymbol{K}^e(\tilde{B}) &= \int_{\Omega^e} (\nabla \times \boldsymbol{N}) \cdot \tilde{A} \cdot (\nabla \times \boldsymbol{N}) \mathrm{d}\Omega \\
\boldsymbol{M}^e(\tilde{A}) &= \int_{\Omega^e} k_0^2 \boldsymbol{N} \cdot \tilde{B} \cdot \boldsymbol{N} \mathrm{d}\Omega \\
\boldsymbol{B}^e(f(\rho), A, B) &= f(\rho^e) j k_0 \int_{\Gamma^e} (\boldsymbol{n} \times \boldsymbol{N}) \cdot \sqrt{AB} \cdot (\boldsymbol{n} \times \boldsymbol{N}) \mathrm{d}\Gamma
\end{aligned}
\tag{10}
$$

where $\boldsymbol{N}$ denotes the shape function. The contributions due to the ABC, free space and incident wave can be computed as described in e.g. [15]. Using the shape functions the objective function can be evaluated by

$$
\Phi(\boldsymbol{H}, \rho) = \bar{\boldsymbol{H}}^T \boldsymbol{Q} \boldsymbol{H}, \quad \text{with } \boldsymbol{Q} = \sum_{e=1}^{N_{obj}} \mu_e \boldsymbol{N}_e^T \boldsymbol{N}_e
\tag{11}
$$

where the overbar denotes complex conjugate and $N_{obj}$ are the number of elements in $\Omega^{obj}$. The optimization problem can be stated on standard form as

$$
\begin{aligned}
\max_{\rho \in \mathbb{R}^N} \quad & \log_{10}(\bar{\boldsymbol{H}}^T \boldsymbol{Q} \boldsymbol{H}) \\
\text{s.t.,} \quad & (\boldsymbol{S}(\rho) + \boldsymbol{A}) \, \boldsymbol{u} = \boldsymbol{f} \\
& \frac{\sum_e^N \rho_e V_e}{V f^*} - 1 < 0 \\
& 0 \le \rho^e \le 1, \quad e = 1, N
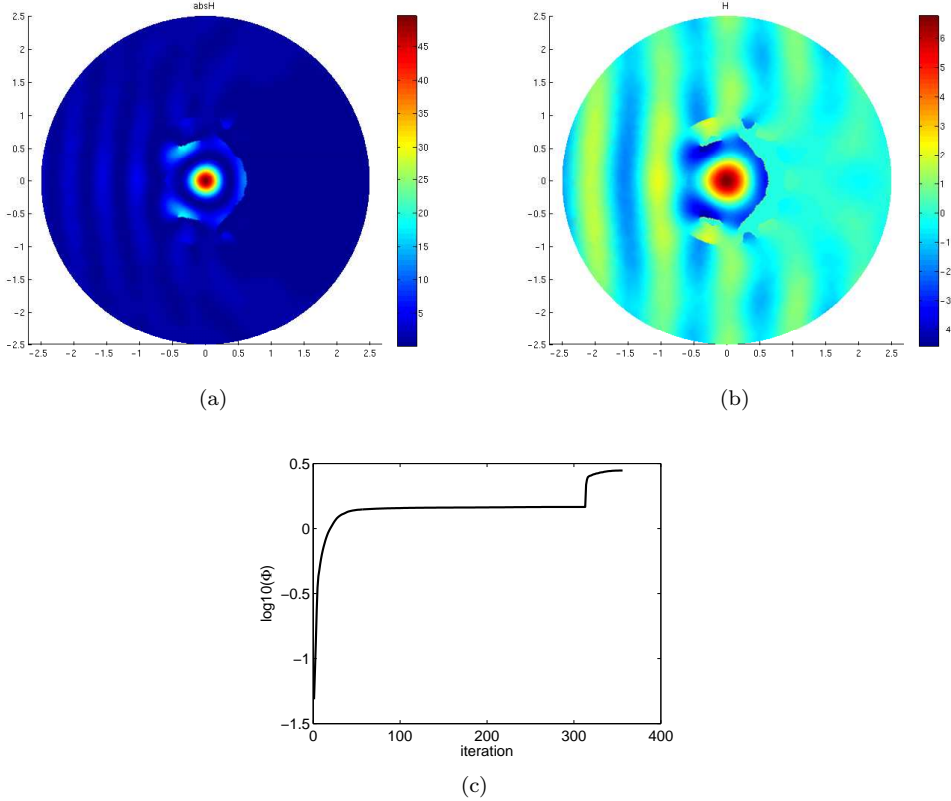\end{aligned}
\tag{12}
$$

6

Figure 4: Plot of the magnetic energy (a), the magnetic field (b) and convergence history (c) associated with the optimized design in figure 3 (c).

where the second constraint is a restriction on the available material used to limit the amount of conductor used for the design problem. The logarithm for the objective is included for proper numerical scaling and the density filter, see [16, 17, 18], is applied to introduce a minimum length scale to the design problem. Since the density filter introduces a region of undesirable intermediate design variables, it is applied in conjunction with a continuation scheme such that the filter radius, $R_{min}$, gradually approaches zero as the optimization process progresses. The optimization problem is implemented in Matlab using triangular nodal and edge based finite elements. The optimization problem is solved using gradient based optimization algorithm the method of moving asymptotes (MMA) courtesy of K.Svanberg [19]. The sensitivities are obtained using the adjoint method, see [5] for details.

6.1. Optimized Designs

The optimization problem is solved using $\sigma^m = 10^6 S/m$ and $\sigma^d = 10^{-4} S/m$ as candidate materials, i.e. a good conductor in free space. The allowed volume fraction is set to 50% of the design domain and the move limit for MMA is set to 0.3. The initial design is a uniform distribution of material in the design domain with $\rho_{init} = 0.1$ unless else is stated. The optimized designs shown in figure 3 are obtained using a two step continuation approach for the density filer. First the radius is set to $0.08m$ and upon convergence it is changed to zero and the optimization is continued. The optimized designs in figure 3(a) and (b) are obtained using the same discretization but different formulations of the Maxwell problem. In figure 3(a) the problem is solved for the electric field using edge finite elements, while the problem in figure 3(b) is solved with nodal elements for the scalar magnetic field. The designs are seen to be quantitatively the same with equivalent objectives, though the area to the right of the parabola have different layouts. For the refined meshes the designs are still qualitatively equivalent to the ones determined on the coarse mesh, but with improved objectives. The difference in objective is most likely due to extra freedom associated with the higher number of design variables for the refined meshes. It should be noted that since the incident field propagates from left to right, the influence of the structure behind the parabola is minimal to the performance of the design. A plot of the magnetic field and energy associated with the optimized design in figure 3(c) is shown in figure 4 along with the iteration history.
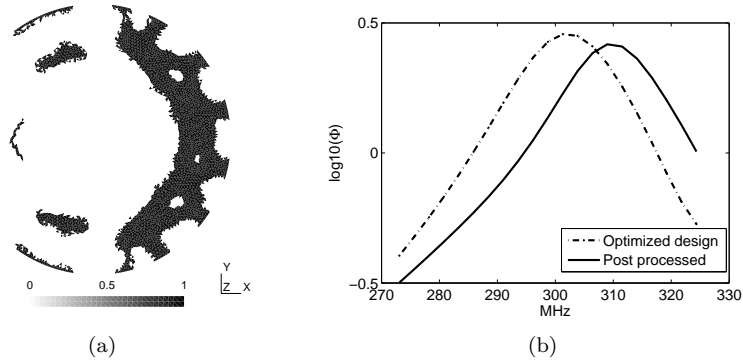
7

Figure 5: Post processing results based on the optimized design of figure 3 (b). The cut off is chosen as $\rho^e > 0.3 \rightarrow 1$ and zero for all other elements. The frequency sweep of the post processed design displays a maximum at 308 MHz with $\Phi = 0.42$, while the optimized design has maximum at 301 MHZ with $\Phi = 0.45$.

From the plot of the magnetic energy, c.f. figure 4(a), it is clear that the energy on the left side of the parabola is close to zero due to shielding effect of the conductor. From the convergence plot in figure 4(c) it is noticed that the convergence is monotone and smooth.

To validate the optimized designs and their performance, the optimized design in figure 3(c) is rendered fully 0-1 by setting all $\rho^e > 0.3$ to one and all others to zero. The now well defined interface between conductor and free space is then modeled by a PEC condition and analyzed by a frequency sweep. The post processed design and plot of the frequency sweep can be seen in figure 5. Here it is noticed that the magnetic energy has a maximum of $\Phi = 0.42$ at 308MHz, while the optimized design shows a maximum at 301MHz of $\Phi = 0.45$. Both objectives are slightly better than the one predicted at 300MHz by the optimized design, but it is especially interesting to see that the target frequency is shifted by 2.7% for the post processed design. This shift in frequency is most likely due to the intermediate design variables in the optimized design. By this is meant that the optimizer can utilize the grey elements to tune the performance of the optimized design to the specified target frequency. When the intermediate design variables are removed during post processing, it then leads to a shift in target frequency and to a small change in objective value. Thus, to circumvent this issue a better filter and/or a combined approach in which the topology optimization is followed by shape optimization should be applied.

## 7. Conclusion

In this paper we have developed a novel design parametrization, based on the interpolation between Maxwell's wave equation and an element impedance condition, which allows for numerically efficient topology optimization of EM metallic microwave devices.

The design parametrization is shown to yield field independent designs meaning that equivalent designs are obtained with the electric and magnetic field formulations of Maxwell's equations. However, due to the numerically large values of a good conductor it was found that the method cannot be used for distributing specific conductors, e.g. silver or copper, but should merely to be used for modeling conductor and no conductor. good conductor designs. The validity of the optimized design was confirmed by the post evaluation in which the optimized design is rendered completely black and white. The now well-defined interface between conductor and dielectric was then modeled by a PEC condition. This analysis showed good agreement with the optimization results, though a shift in peak frequency was observed. The shift is contributed to presence of intermediate design elements in the optimized design. This means that either a better filtering technique should be applied, or the topology optimization should be followed by a few iterations of a shape optimization scheme.

A more elaborate paper on this work, including several other examples, has been submitted as a journal article.

8

## 8. References

[1] Balanis C.A. *Antenna Theory: Analysis and Design* (3rd edn) John Wiley & Sons., 2005

[2] Kurs A., Karalis A., Moffatt R., Joannopoulos J.D., Fisher P. and Soljacic M. Wireless power transfer via strongly coupled magnetic resonators. *Science* 2007; **317**

[3] Bendsøe M. P. and Kikuchi N., Generating optimal topologies in structural design using a homogenization method, *Comput. Methods Appl. Mech. Eng.* 1988, **71**:197-224

[4] M.P. Bendsøe and O. Sigmund, *Topology Optimization: Theory, Methods and Applications*, Springer-Verlag, Berlin, 2003.

[5] J. Jensen and O. Sigmund, Topology optimization of photonic crystal structures: a high-bandwidth low-loss T-junction waveguide, *Journal of the Optical Society of America* 2005, **22**(6)

[6] Borel P. I., Harpth A., Frandsen L. H., Kristensen M., Shi P., Jensen J. S., and Sigmund O., Topology optimization and fabrication of photonic crystal structures, *Optical Express* 2004, **12**:1996-2001.

[7] Kiziltas G., Kikuchi N., Volakis J.L. and Halloran J., Topology optimization of dielectric substrates for filters and antennas using SIMP, *Archives Of Computational Methods In Engineering* 2004, **11**(4):355–388

[8] Erentok A. and Sigmund O., Topology optimized efficient sub-wavelength antennas with large bandwidth, SUBMITTED

[9] Koulouridis S., Psychoudakis D. and Volakis J.L., Multiobjective Optimal Antenna Design Based on Volumetric Material Optimization, *IEEE Transactions on antennas and propagation* 2003, **55**(3):594–603

[10] Balanis C.A. *Advanced Engineering Electromagnetics* (1st edn) John Wiley & Sons Inc., 1989

[11] Jin J. *The Finite Element Method in Electromagnetics* (2nd edn) John Wiley & Sons., 2002

[12] Zhu Y. and Cangellaris A. *Multigrid Finite Element Methods for Electromagnetic Field Modeling* (1st edn) John Wiley & Sons., 2006

[13] Bendsøe, M. P., Optimal shape design as a material distribution problem, *Structural Optimization* 1989, **1**:193–202.

[14] Diaz A. R. and Sigmund O., Negative permeability metamaterial design by topology optimization, SUBMITTED

[15] Jin J. and Riley D.J. *The Finite Element Analysis of Antennas and Arrays* (1st edn) John Wiley & Sons., 2008

[16] Bourdin B., Filters in topology optimization. *International Journal for Numerical Methods in Engineering* 2001, **50**(9):2143-2158

[17] Bruns T.E. and Tortorelli D.A., Topology optimization of nonlinear elastic structures and compliant mechanisms. *Computater Methods in Applied Mechanics and Engineering* 2001, *190*(26-27):34433459

[18] Sigmund O., Morphology-based black and white filters for topology optimization, *Structural and Multidisciplinary Optimization* 2007, **33**:401–424

[19] Svanberg K., The method of moving asymptotes - a new method for structural optimization, *International Journal for Numerical Methods in Engineering* 1987, **25**